RESEARCH PAPER

A Compact Reconfigurable CPW-Fed Dual Band-Notched UWB Antenna Using PIN Diodes

Koduri Sreelakshmi[1] [ORCID] · **Gottapu Sasibhushana Rao[2]**

Abstract

A compact printed monopole UWB antenna with the capability of reconfigurable notched bands using dual PIN diodes is introduced and fabricated. The proposed antenna comprises a patch with a U-shaped aperture, two parasitic rectangular stubs, and embedded two metamaterial rectangular complementary split ring resonator (CSRR) structures. The investigated antenna has a compact size of 24×20 mm^2 and is modeled on a FR-4 substrate that is 0.787 mm thick. The presented antenna rejects interference with S-band (2.85–3.34 GHz) and the WLAN (4.9–5.64 GHz). The investigated UWB antenna reconfigurability is realized by inserting two PIN diodes within the CSRR configurations to realize four distinct characteristics, specifically UWB characteristics, single band-notch UWB characteristics at WLAN, single band-notch UWB characteristics at S-band, and dual band-notch UWB characteristics at S-band and WLAN. The measured results in the first case demonstrate that the presented UWB antenna provides service throughout a range of frequencies from 2.7 to 11.4 GHz, with a fractional impedance bandwidth of 123.4% for VSWR $\leq$ 2. The performance of antenna is investigated in both frequency and time domains. The investigated antenna prototype model is built and tested to verify its desirable characteristics. The investigated antenna is more relevant for UWB reconfigurable band-notch applications with the good similarity between measured and simulated results.

Keywords Band notch · CSRR · S-band · UWB · WLAN

1 Introduction

Ultra-wideband (UWB) system has become increasingly popular by virtue of its larger bandwidth which provides several benefits including reduced power consumption than the current system, improved data rate, compatibility with narrowband systems, opposition to interference, and especially cost-effective implementation (Valderas et al. 2011) for several different UWB applications. A system is considered ultra-wideband (UWB) if it either uses 500 MHz of the spectrum or has a fractional bandwidth of at least 20%.

UWB research began in 1893 when Hertz performed an experiment on UWB; however, in February 2002, the design of UWB antenna gained prominence when the Federal Communication Commission (FCC) assigns the license-free frequency spectrum of 3.1–10.6 GHz for UWB applications (Federal Communications Commission 2002) (Schantz 2005). These alluring characteristics of UWB technology have drawn numerous researchers to create and design UWB antennas appropriate for UWB communication, as detailed in Ray (2008) (Galvan-Tejada et al. 2015). The requirements of the UWB antenna are omnidirectional radiation characteristics, good gain, compact size, and wide bandwidth. However, the UWB frequency overlaps with many licensed frequency bands such as S-band and WLAN. These license bands must be separated from the UWB frequency band, necessitating the use of frequency blocking designs in the proposed structure of antenna. The antenna, along with filtering operation, is famous as filtering-antenna or filtenna. Filtenna has various benefits, including reduced losses, low cost, and miniature size. Two

✉ Koduri Sreelakshmi
  lakshmisaibaba12@gmail.com

  Gottapu Sasibhushana Rao
  sasigps@gmail.com

[1] Department of ECE, Anil Neerukonda Institute of Technology and Sciences (A), Vishakhapatnam, India

[2] Department of ECE, Andhra University College of Engineering (A), Andhra University, Vishakhapatnam, India

Springer

main challenges while fabricating frequency blocking configurations are their shape and placement.

Earlier investigations have proposed a huge number of single, double, and triple band-notch UWB antennas such as by embedding: the radiating structure with four circular patch-loaded stubs and two CSRRs on the ground plane (Puri et al. 2020), one horizontal and 2 split ring apertures in the structure of patch (Sharma and Bhatia 2019), split ring-shaped and V-shaped slit on antenna (Bong et al. May 2019), slits and one pair of λ/2 stubs inside the circular patch and tapered slot aperture (Shi et al. 2018), U-shaped aperture, meandered aperture, and E-shaped stub within the antenna (Iqbal et al. 2019), aperture of U-shape in the transmission line and meandered aperture on the patch (Sohail et al. 2018), aperture with the shape of elliptical ring and 2 slits of S-shape in the antenna design (Emadian and Ahmadi-Shokouh Oct. 2015), 3 C-shaped apertures within the patch (Hammache et al. Jan. 2019), H-shaped resonator besides feed line (Sung Feb. 2013), a strip of T-shape within the patch and strip of U-shape near the transmission line (Jiang and Che 2012), the SRR slots on a radiating patch and placing two rectangular metamaterial SRR's next to the feed (Jairath et al. 2021), aperture of S-shape within the feed line and an asymmetrical parasitic stub of C- shape just above the DGS (V. N. Koteswara Rao Devana and A. Maheswara Rao" 2020), the hexagonal slot (Parameswari 2021), a triangular slot, three split-ring resonators of square shape onto the radiating patch (Vallappil et al. 2022), and a low profile UWB triple band-notch antenna fed with microstrip line (Sarkar et al. 2014). However, these antennas (Puri et al. 2020; Sarkar et al. 2014) cover the entire UWB frequency range, but they have inflexible band-notch characteristics, and they are not deploying overall UWB frequency range when there is no obstruction from notched bands, i.e., they lack reconfigurability. Hence, employing reconfigurable notch-band configuration (Costantine et al. March 2015) can enhance the functioning of the UWB system. Currently, various antennas with reconfigurable band-notch characteristics are investigated such as integrating: a single varactor / capacitor onto a resonant slot (Antonino-Daviu et al. 2007) (Hu et al. 1588), PIN diodes at appropriate places (Oraizi and Shahmirzadi 2017), MEMS switches onto U-shaped slot and inverted L-shaped stub(Nikolaou et al. 2009), multiple varactors and PIN diodes onto S-shaped SRR (Horestani et al. 2016), four switches onto TS-TSIR and PSLR (Li et al. 2014), single varactor onto annular slot (Hua et al. 2017), two PIN diodes onto two DSRR (Alhegazi and Zakaria 2017), three PIN diodes among parasitic strip, circular ring and stub of T-shape (Kalteh et al. 2012), two OCMSs onto CSRRs etched in radiation structure (Zhao et al. 2014), shorting plates onto aperture of C-shape on the feed line and arc-shaped aperture on patch (Ting

et al. 2014), by connecting the main feed line with four stubs employing GaAs FET switches (Aboufoul et al. 2012), single PIN diode onto ST-SRR structure on feed line (Lakrit et al. 2019), single varactor onto slot in microstrip line (Mohamed et al. 2017). By adjusting the size of the open-ended L-shaped slot (De et al. 2020), by etching on both sides of feed line a pair of double split ring resonators (DSRRs) and the radiating element with inverted pi-slot (Mayuri 2020), and by employing three elliptical slots (Elkorany et al. 2021), by etching circular patch with an annular slot and a semi-elliptical slot on which is loaded with a varactor diode (Moradi and Nazari 2022). But these antennas (Costantine et al. March 2015; Moradi and Nazari 2022) have large dimensions, complex structures, fails cost–efficient design as they use expensive substrate materials and multiple active components.

In this letter, a compact reconfigurable dual band-notch UWB filtenna is examined. The investigated filtenna configuration is simulated using a commercial electromagnetic simulation platform HFSS v 19. Various configurations of PIN diodes are simulated to validate the reconfigurable band-notch characteristics. The paper is well organized, covering various existing methods in UWB band-notch antenna design in the introduction section. Section 2 describes the proposed design's step-by-step implementation, operating principle, and parametric study. In Sect. 3, the simulated performance characteristics are justified using experimental investigation. However, the time-domain response of the investigated antenna is also examined in Sect. 4. In Sect. 5 a performance comparison of the presented work with existing latest literature is carried out to highlight the author's contribution. Lastly, conclusions are provided in Sect. 6.

2 Design Structure of Presented Filtenna

Figure 1 illustrates the investigated UWB filtenna structure with reconfigurable dual band-notched characteristics. The investigated antenna comprises of a radiating patch with a U-shaped aperture, two parasitic rectangular stubs, and embedded two metamaterials rectangular CSRR structures at the center of the radiating patch. The investigated UWB antenna is modeled on an inexpensive FR-4 substrate of thickness 0.787 mm, loss tangent of 0.02, and the dielectric constant of 4.4. The investigated compact UWB filtenna has a substrate size of $24 \times 20 \text{ mm}^2$. The investigated UWB filtenna attained an VSWR bandwidth of 2.64–11.36 GHz and dual notched bands centered at 3.15 GHz (S-band) with the VSWR bandwidth 2.87–3.31 GHz and 5.35 GHz (WLAN) with the VSWR bandwidth 4.92–5.65 GHz. The presented UWB monopole antenna has achieved frequency reconfigurable band-notch
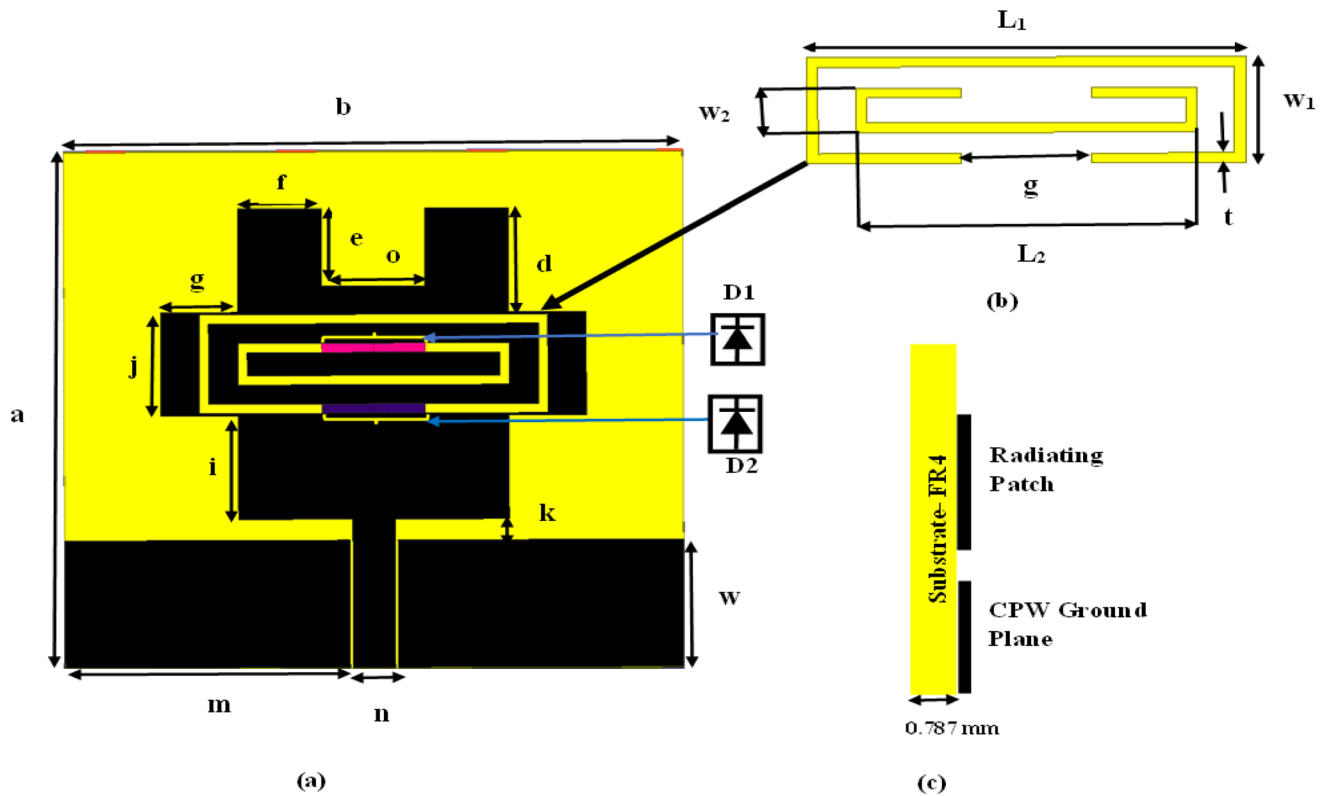
Fig. 1 a Structure of the investigated UWB filtenna, b structure of the presented CSRR, and c side view

characteristics by embedding the CSRR structure with two switching PIN diodes in the center of the monopole patch. The optimal dimensions of the investigated UWB filtenna are shown in Table 1.

Figure 2 demonstrates the investigated UWB filtenna step-by-step development. Antenna-I configuration is obtained by considering the printed rectangular monopole antenna (PRMA) to achieve UWB response. The ground plane on back side of PRMA is located at infinity which is a special case of rectangular microstrip antenna structure.

Table 1 Investigated antenna dimensions

Parameters	Values (mm)	Parameters	Values(mm)
a	24 mm	f	3.25 mm
b	20 mm	e	3 mm
m	11.075 mm	o	4 mm
n	1.65 mm	g	4 mm
w	5 mm	k	0.8 mm
i	4 mm	j	4 mm
d	4 mm	L_1	13.5 mm
w_1	3.8 mm	L_2	10.5 mm
w_2	1.6 mm	t	0.35 mm
g	4 mm		

Antenna-1 structure includes rectangular patch which is placed on one side of substrate (FR4). It can be assumed that an extremely thick air dielectric substrate ($\varepsilon_r = 1$) exists on other side of substrate. It creates a microstrip patch antenna structure on a thick substrate with ε_r near unity, resulting in a large bandwidth.

The design parameters of the rectangular radiating patch are initially estimated using an empirical relation of lower cut-off frequency defined by Eq. (1), respectively (Ray 2008).

$$f_L = \frac{7.2}{\left(L_P + \frac{W_P}{2\pi} + K\right) \times P} \text{GHz} \tag{1}$$

$$\varepsilon_{reff} = \frac{\varepsilon_r + 1}{2}$$

f_L lower cut-off frequency (GHz)
    L_P Length of the patch (cm)
    W_P width of the patch (cm)
    k feed gap (cm)

where $P = \sqrt{\varepsilon_{reff}}$ and it helps to calculate the dielectric substrate impact on the lower cut-off frequency. Antenna-I operates over UWB range of 3.15–10.17 GHz with VSWR $\leq$ 2 as illustrated in the VSWR characteristics of Fig. 3. In the design process second step (Antenna-II), two rectangular stubs are inserted on both sides along the length

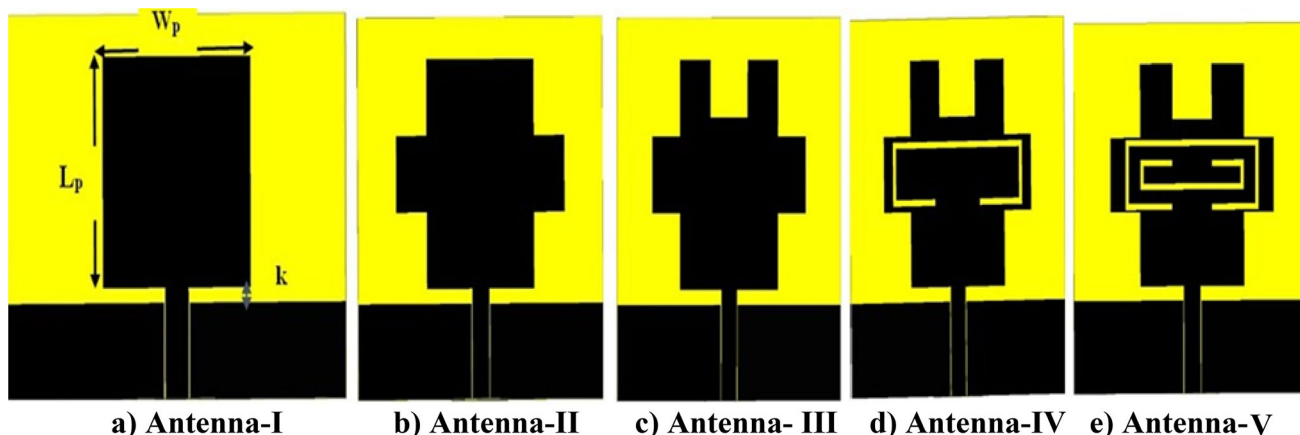a) Antenna-I   b) Antenna-II   c) Antenna- III   d) Antenna-IV   e) Antenna-V

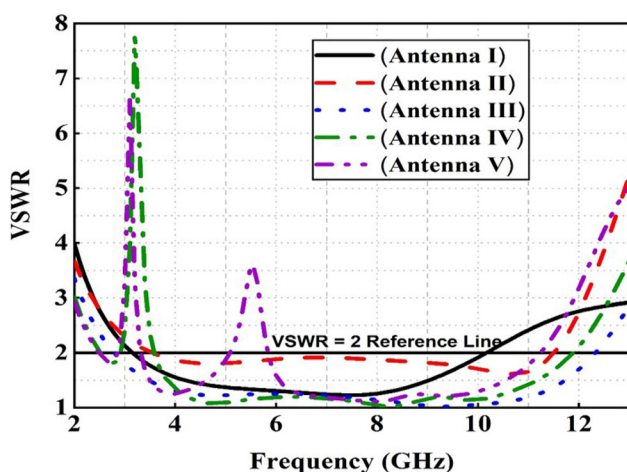Fig. 2 Development of the investigated UWB filtenna in stages

Fig. 3 Simulated VSWR characteristics at different steps in antenna evolution

of the patch to enhance the VSWR bandwidth of the investigated UWB filtenna. The VSWR characteristics are illustrated in Fig. 3 for Antenna-II which indicates that the bandwidth of the investigated UWB filtenna is increased by 950 MHz, resulting in VSWR ≤ 2 from 3.54 to 11.51 GHz. In the subsequent step (Antenna-III), U-shaped aperture is cut from the upper edge of the patch to further improve the operating bandwidth of the investigated UWB antenna. Figure 3 illustrates that by employing the antenna-III the impedance bandwidth is further enhanced by 1570 MHz, resulting in VSWR ≤ 2 from 2.79 to 12.33 GHz.

In the fourth step (Antenna-IV), CSRR#1 is etched at the center of investigated PRMA to eliminate frequencies that UWB and S-band systems can interfere with. Figure 3 illustrates that the Antenna-IV continues to operate in the UWB range of 2.51–11.89 GHz with VSWR ≤ 2 and exhibits notch at S-band from (2.91–359 GHz) with VSWR > 2. Finally (Antenna-V), to eliminate frequencies

that UWB and WLAN systems can interfere with, the inner most CSRR#2 is embedded at the center of investigated PRMA. As illustrated in Fig. 3, Antenna-V shows the UWB response over 2.48–11.24 GHz with VSWR ≤ 2 and exhibits two sharp stop bands (VSWR > 2) at S-band and WLAN frequencies, the first notch band is achieved from 2.86 to 3.32 GHz and second band is achieved from 5.08 to 5.84 GHz. Similarly, the parameters of the two CSRR configurations are predicted using Eqs. (2–4), respectively (Sarkar et al. 2014). The notch frequency can be appropriately adjusted by modifying the length of the two split ring-shaped slots.

$$f_{\text{in}} = \frac{c}{2S^i_{\text{CSRR}}\sqrt{\varepsilon_{\text{reff}}}} \tag{2}$$

where

$$s^i_{\text{CSRR}} = 2(L_i + W_i) - g \tag{3}$$

$$\varepsilon_{\text{reff}} = \frac{\varepsilon_r + 1}{2} \tag{4}$$

Here, c is the speed of light in free space, f_{in} is ith notch frequency (where $i = 1$ and 2 for CSRR #1 and CSRR #2), $\varepsilon_{\text{reff}}$ is the effective relative permittivity, and S^i_{csrr} is the total length of ith CSRR. Table 2 presents a simulated performance evaluation of the examined antenna under various evolution scenarios.

To realize the frequency reconfigurable band-notch characteristics, dual PIN diodes (BA482 from Philips) are embedded in the investigated antenna. A series combination of inductance ($L = 0.6$ nH) and resistance ($R_S = 1$ Ω) is used to depict the RF PIN diode in its ON position (forward bias). It is depicted as a parallel connection of the capacitor ($C_T = 0.1$ pF) and resistor ($R_P = 0.1$ KΩ) with an inductor ($L = 0.6$ nH) in series, while it is in the OFF state (reverse bias). Figure 4a depicts an equivalent circuitry representation of a PIN diode. In HFSS simulation, diode is represented using the resistance, inductance, and

Table 2 Simulated performance evaluation of the examined antenna

Configuration	Operating frequency range (GHz)	Impedance bandwidth (GHz)	Fractional bandwidth FBW%	Notch bands	Notched bandwidth (GHz)
Antenna-I	3.15–10.17	7.02	105.4	–	–
Antenna-II	3.54–11.51	7.97	111	–	–
Antenna-III	2.79–12.33	9.54	126.2	–	–
Antenna-IV	2.51–11.89	9.38	130.3	S-band	2.91–3.59
Antenna-V	2.48–11.24	8.76	127.7	S-band, WLAN	2.86–3.32, 5.08–5.84
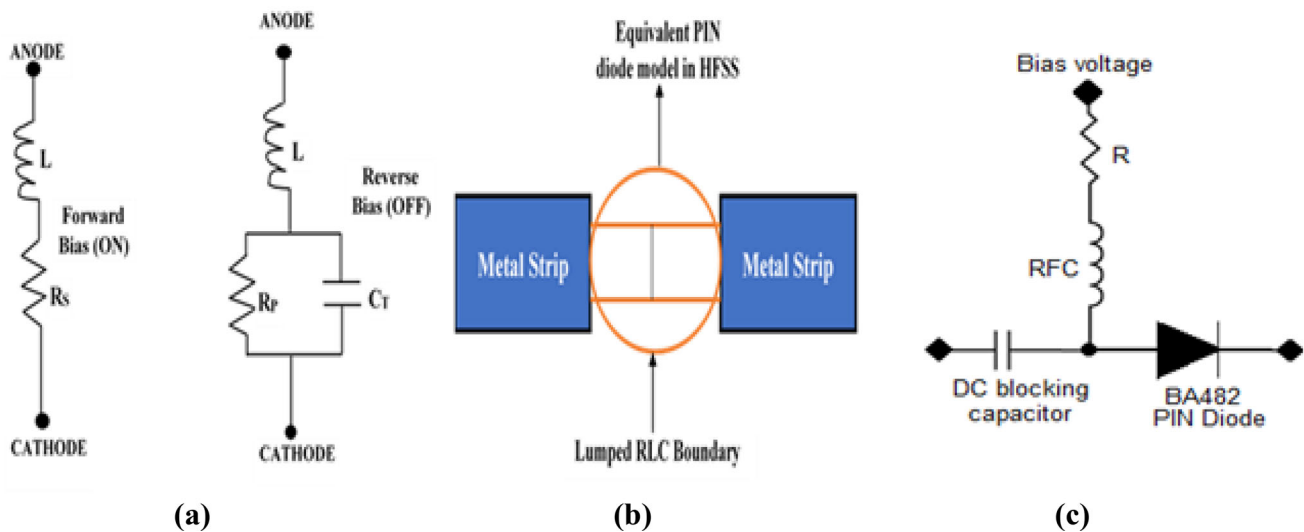
Fig. 4 PIN diode electrical model; **a** equivalent model using lumped elements, **b** model in HFSS, and **c** biasing circuit

capacitance (RLC) boundary by introducing two rectangular sheets in the diode position as shown in Fig. 4b. To switch ON and OFF, the PIN diodes D1 and D2; the bias voltage of 5 and 0 V is applied. By adding an RF inductor of 33 nH from coil craft in series with the bias line, an RF by-pass capacitor of 10 pF from Murata in series with the RF input the DC bias supply is isolated from the RF circuits and the circuit is connected to regulated supply of 5 V as illustrated in Fig. 4c.

2.1 Parametric analysis

To investigate how the UWB filtenna performs when the CSRR's dimensions are changed, a complete parametric investigation has been conducted in the HFSS software. Figure 5a demonstrates how parameter L_2 affects the VSWR of the proposed UWB filtenna. When L_2 was enhanced from 10.5 to 11 mm, the upper notch band (WLAN) shifted to the lower frequency, while the lower band-notch (S-band) remained constant. The upper band-notch frequency was observed at 5.4 GHz for $L_2 = 11$ mm,

and changing the value of L_2 from 10.5 to 10 mm shifted the upper band-notch frequency from 5.5 to 5.6 GHz. This is due to the inverse relation in between the length of the inner CSRR and the band-notch center frequency. Figure 5b demonstrates how parameter L_1 affects the VSWR of the proposed UWB filtenna. The L_1 parameter controls the notch at the lower band (S-band) of the investigated antenna. The lower band-notch frequency was observed at 3.0 GHz for $L_1 = 14$ mm and changing the value of L_1 from 13.5 to 13 mm, shifted the lower band-notch frequency from 3.1 to 3.3 GHz. This is due to the inverse relation in between the length of the outer CSRR and band-notch center frequency. Furthermore, it is shown that by changing one of these dimensions, just the corresponding notched frequency band shifts without impacting the other notched band, showing that the two notched bands almost have no influence on one another and are independently adjustable. This property provides significant flexibility in designing and controlling the notched frequency bands of the investigated UWB filtenna.
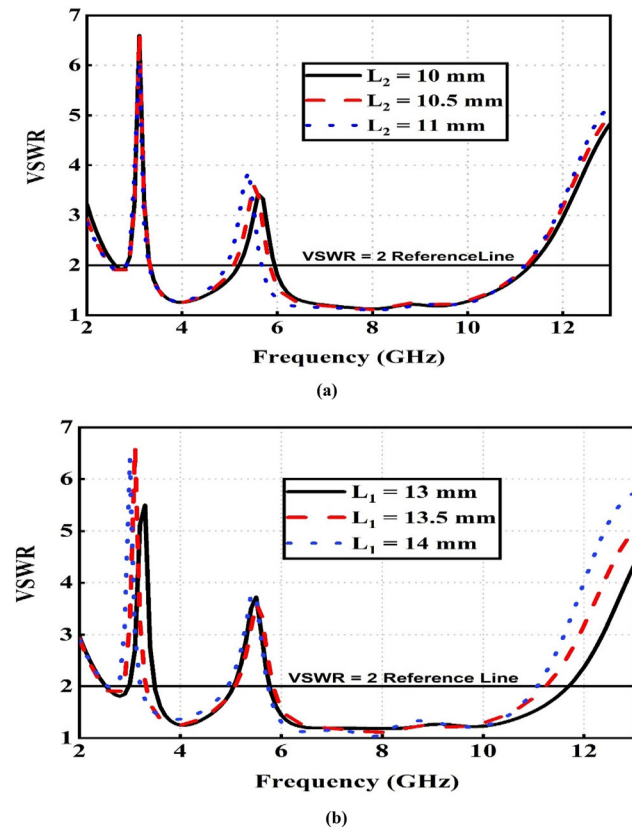
(a)

(b)

Fig. 5 Controllable notch bands by varying **a** L_2 and **b** L_1
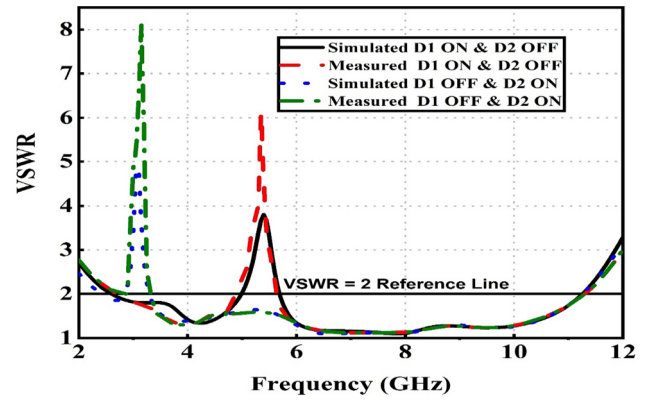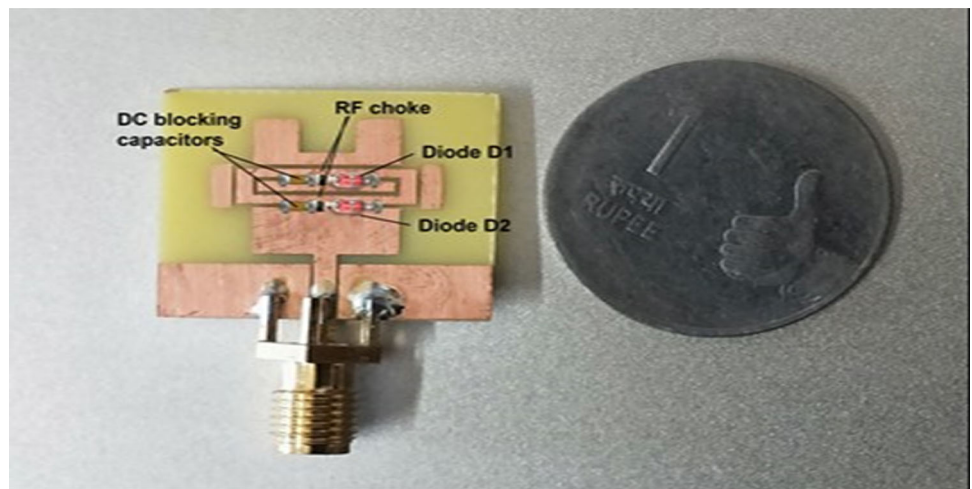

Fig. 7 Measured and simulated VSWR for the various operating modes for PIN diodes in Mode 1 and Mode 2

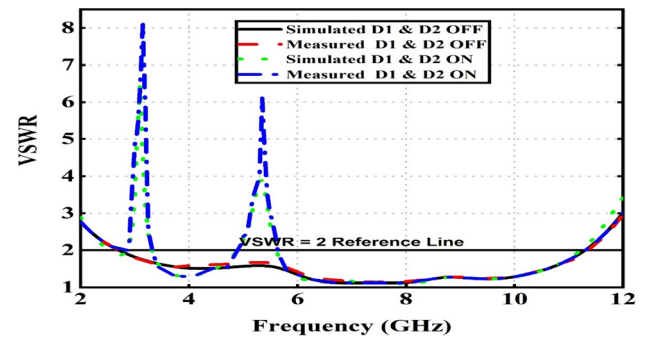**Fig. 8** Measured and simulated VSWR for the various operating modes for PIN diodes in Mode 3 and Mode 4

3 Results and Discussion

To validate the simulated results obtained from HFSS, the proposed antenna is fabricated and antenna prototype is illustrated in Fig. 6. The VSWR measurements are taken using a calibrated Agilent Fieldfox N9916A 14 GHz Handheld RF Vector Network Analyzer. Dual PIN diodes (D1 and D2) are used for possible four modes of operation of the proposed UWB filtenna.
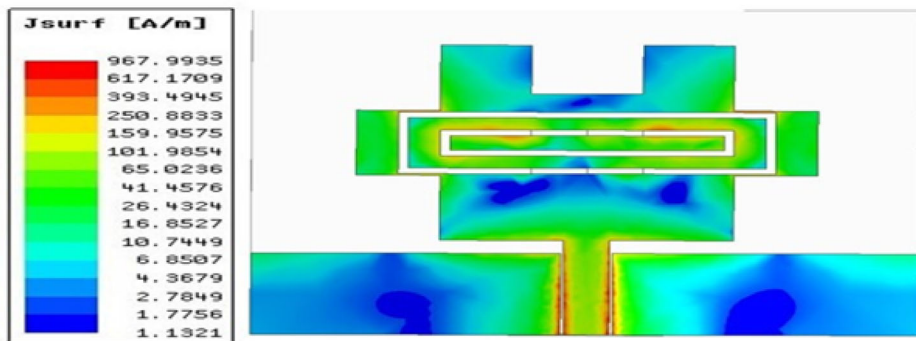
3.1 Mode 1

When PIN diode D1 is switched ON and D2 is switched OFF, the investigated filtenna operates in Mode 1. Figure 7 demonstrates the measured and simulated VSWR characteristics of the investigated filtenna in this mode. The

Fig. 6 Fabricated prototype of the presented UWB filtenna
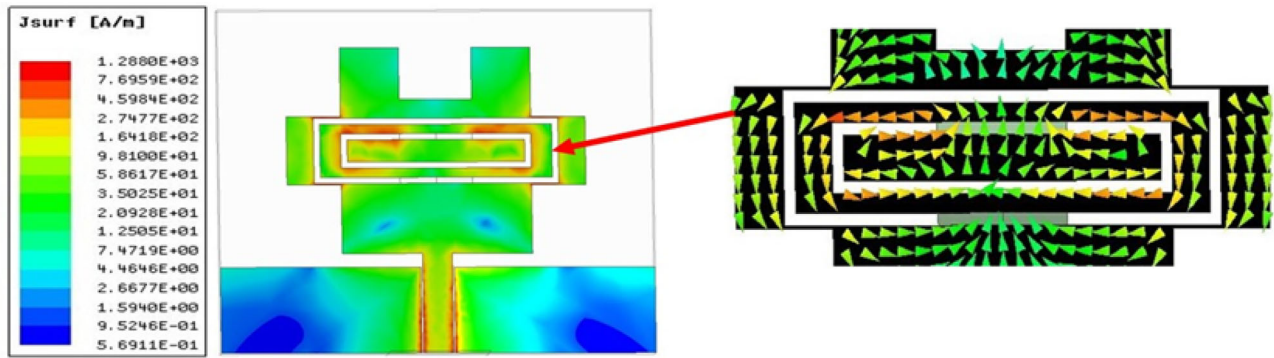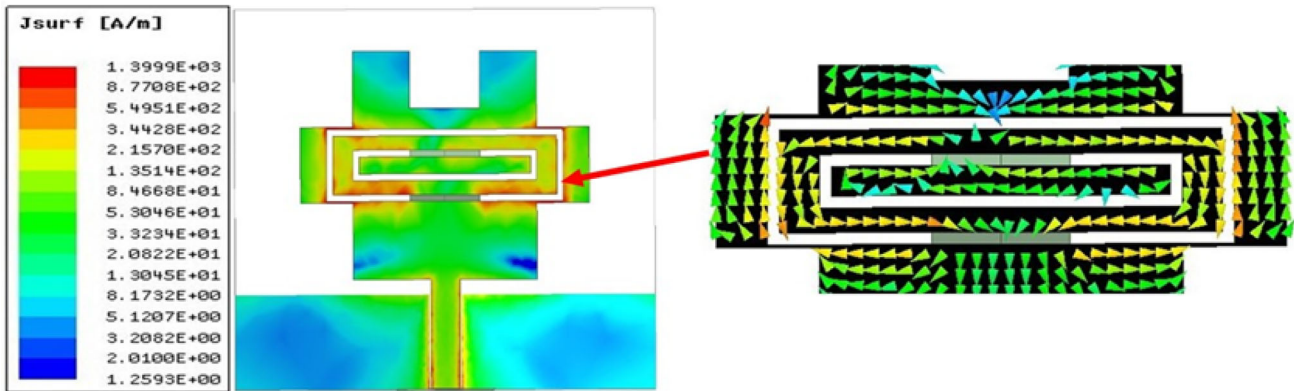
Fig. 9 Distribution of surface current of the presented filtenna at frequencies: **a** 5.5 GHz (Mode 1), **b** 3.5 GHz (Mode 2), and **c** Mode 3

investigated filtenna operates at wide bandwidth (VSWR ≤ 2) from 2.65 to 11.35 GHz with single band notch (VWSR > 2) at 5.35 GHz to avoid interference with WLAN applications. The current distribution at the band-notch frequency 5.35 GHz is depicted in Fig. 9a. The current is obviously significantly focused on the inner CSRR and flows in opposing directions at adjacent walls with a similar magnitude, canceling each other out and resulting in high attenuation. As a result of this, the filtenna

does not emit radiation and a band notch at 5.35 GHz is formed.

3.2 Mode 2

When PIN diode D1 is switched OFF and D2 is switched ON, the investigated filtenna operates in Mode 2. Figure 7 demonstrates the measured and simulated VSWR characteristics of the investigated filtenna in this mode. The investigated antenna operates at wide bandwidth (VSWR
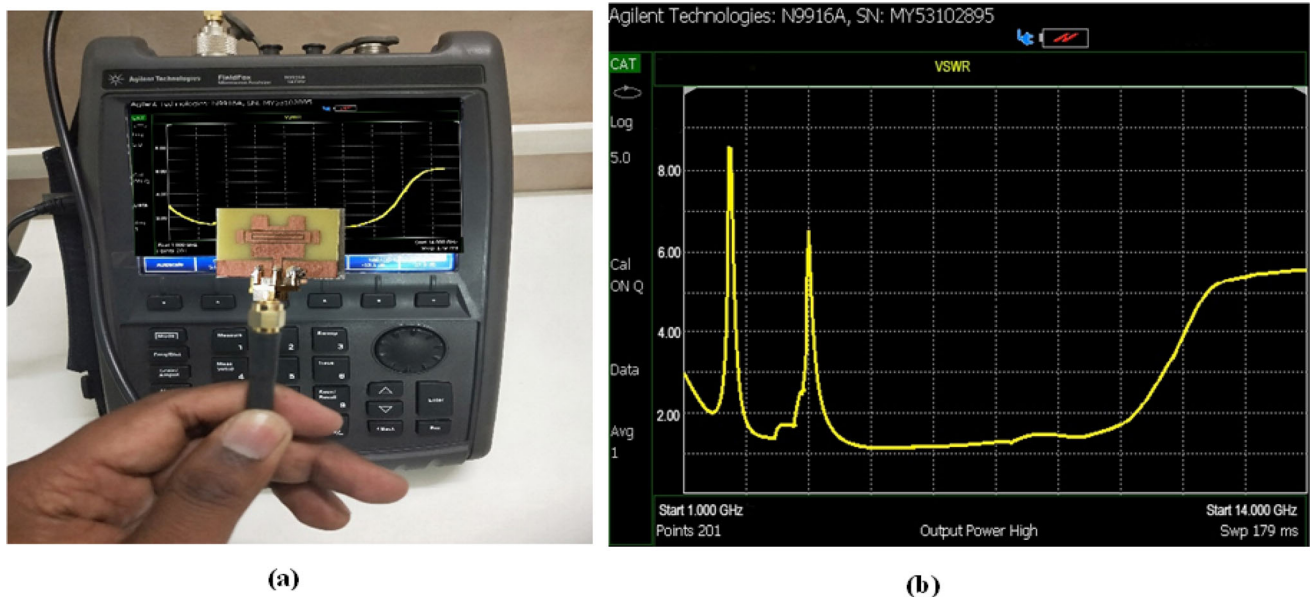
Fig. 10 Measurement carried out on VNA to validate results **a** for both PIN diodes OFF and **b** for both PIN diodes ON

Table 3 Summary of investigated antenna reconfigurable band-notch switching

Model	Mode	D1	D2	−10 dB bandwidth (GHz)	Bandwidth (%)	Notch (GHz)	Notched bandwidth (GHz)
Simulated	1	ON	OFF	2.59–11.26	125.2	5.4 (WLAN)	4.99–5.69
	2	OFF	ON	2.41–11.26	129.5	3.1 (S-band)	2.85–3.3
	3	OFF	OFF	2.7–11.31	122.9	None (UWB antenna)	None (UWB antenna)
	4	ON	ON	2.52–11.23	126.7	3.1 (S-band), 5.5 (WLAN)	2.85–3.32, 4.89–5.61
Measured	1	ON	OFF	2.65–11.35	124.3	5.35 (WLAN)	4.9–5.63
	2	OFF	ON	2.58–11.33	125.8	3.15 (S-band)	2.88–3.32
	3	OFF	OFF	2.68–11.38	124.6	None (UWB antenna)	None (UWB antenna)
	4	ON	ON	2.64–11.36	124.6	3.15 (S-band), 5.35 (WLAN)	2.87–3.31, 4.92–5.65

≤ 2) from 2.58 to 11.33 GHz with single band notch (VWSR > 2) at 3.15 GHz to avoid interference with S-band applications. The current distribution at the band-notch frequency 5.35 GHz is depicted in Fig. 9b. It is evident that the current is much more concentrated on the outer CSRR and that the adjacent walls have opposing current directions, resulting in a band-stop effect at 3.15 GHz.

3.3 Mode 3

When the diodes D1 and D2 are switched OFF, the proposed antenna functions in Mode 3. Figure 8 depicts the measured and simulated VSWR characteristics of the investigated filtenna in this mode. The investigated antenna in this mode provides UWB operation (VSWR ≤ 2) over the frequency range 2.68–11.38 GHz without band notches. Figure 9c depicts the current distribution of the proposed UWB filtenna in this mode at 5.5 GHz. It is clearly seen when both the diodes are OFF, the effect of CSRR disappears. So, the corresponding notched bands are removed.

3.4 Mode 4

When the diodes D1 and D2 are switched ON, the proposed antenna functions in Mode 4. Figure 8 demonstrates the measured and simulated VSWR characteristics of the investigated filtenna in this mode. The investigated filtenna operates at wide bandwidth (VSWR ≤ 2) from 2.64 to 11.36 GHz with dual band notches (VWSR > 2) at 3.15 and 5.35 GHz to avoid interference with S-band and WLAN applications.
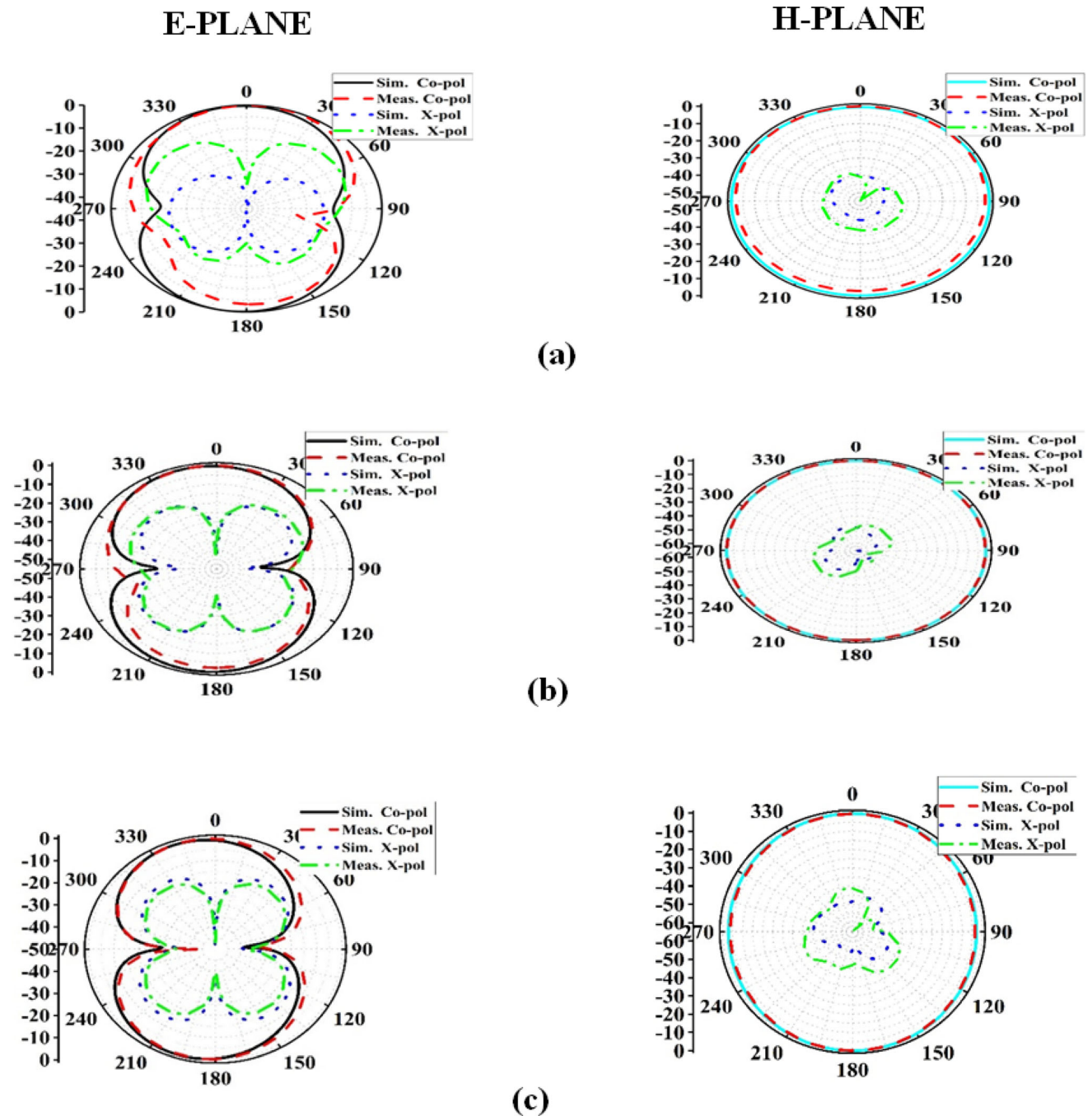
Fig. 11 Radiation characteristics along E-plane and H-plane; **a** 3.5 GHz, **b** 6.5 GHz, and **c** 8.5 GHz

Figure 10 illustrates a snapshot of the VNA 9916A from Agilent Fieldfox with the investigated UWB filtenna measured VSWR characteristics. There is a minor difference between measured and simulated VSWR, which could be caused by errors in soldering the PIN diodes, during antenna manufacturing, and losses because of cable connecting measuring devices and antenna. Table 3 summarizes the different band notches achieved by the switching

mechanism of the diodes D1 and D2 during simulation and measurement.

The investigated UWB filtenna measured and simulated radiation 2D patterns at 3.5, 6.5, and 8.2 GHz in E-plane and H-plane is presented in Fig. 11a–c. Moreover, it is noticed that the investigated UWB filtenna possesses omnidirectional radiation characteristics within the H-plane and relatively directional radiation characteristics in the E-plane, almost like a standard monopole. The
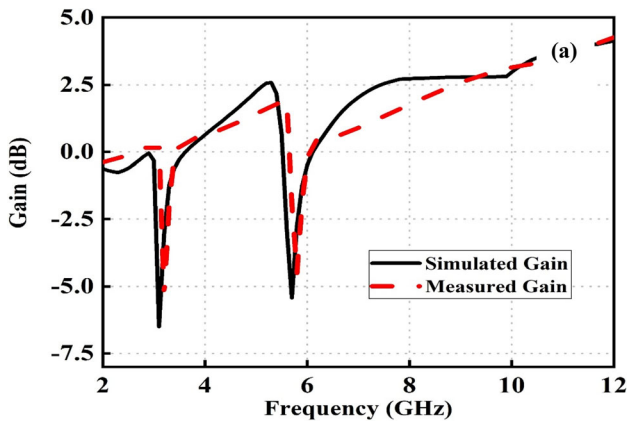
Fig. 12 Simulated and measured gain of the investigated UWB filtenna

simulated and measured gain plot of the investigated fil-tenna for mode 4 operation is illustrated in Fig. 12. The measured gain is minimum at 3.2 GHz (− 5.3 dBi) and maximum at 12.5 GHz (4.4 dBi) and at the specified band-notches at 3.15 and 5.35 GHz, there is a sharp reduction in gains which validates the elimination of interference sig-nals out of S-band and WLAN systems.

4 Time Domain Analysis

The UWB system employs very narrow time pulses (< 2 ns) to cover a wide frequency spectrum. Because narrow pulses are heavily influenced by dispersion, the radiating pulse will differ from the input pulse of the antenna. To estimate the distortion generated by the investigated antenna, a time-domain evaluation of the
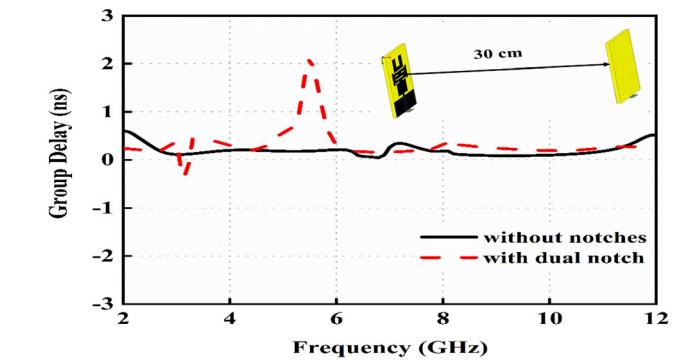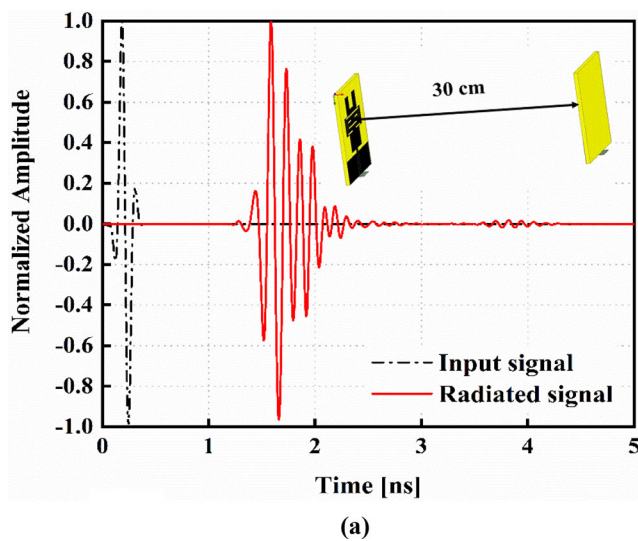

Fig. 14 Simulated group delay of the investigated antenna when arranged face to face for Mode 3 and Mode 4
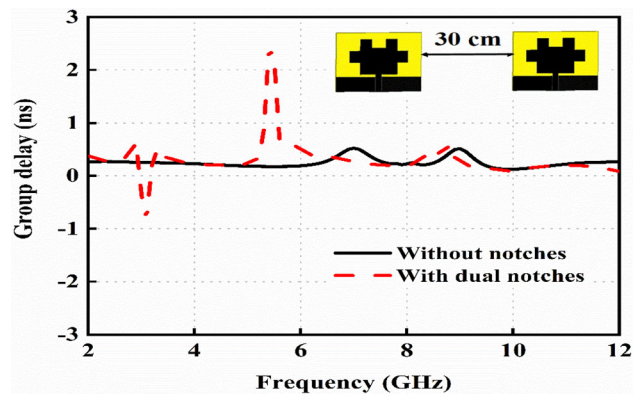

Fig. 15 Simulated group delay of the investigated antenna when arranged side by side for Mode 3 and Mode 4

transmitted pulse is performed. HFSS software is employed to obtain the time domain response of the investigated antenna. The two similar structures of the investigated
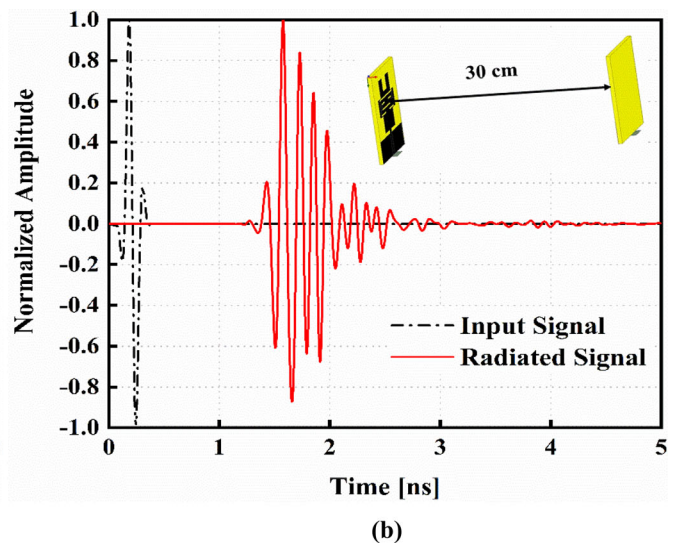

Fig. 13 Normalized input and radiated signals of the investigated antenna for **a** Mode 3, **b** Mode 4 (R = 30 cm)

Table 4 Comparison of existing work with proposed work

References	Size (mm³) and volume (mm³)	Substrate	Frequency coverage (GHz)	FBW (%)	Notch bands (GHz)	Switching capability	No of active components integrated
Puri et al. 2020)	32 × 30 × 1.6 1536	FR4	2.76–11	119.7	2(4.4, 5.8)	No	NA
Sharma and Bhatia 2019)	30 × 30 × 1.6 1440	FR4	2.45–12	132	2(5.4, 7.4)	No	NA
Iqbal et al. 2019)	33 × 34 × 1.6 1795	FR4	1.4–11.3	156	3(2,3.5, 5.8)	No	NA
Sohail et al. 2018)	33 × 32 × 1.5 1584	FR4	2–11	138.4	2(3.5, 5.6)	No	NA
Vallappil et al. 2022)	28 × 40 × 1.6 1792	FR4	3–12	120	2(4.75, 7.7)	No	NA
Ting et al. 2014)	38 × 25 × 1.6 1520	FR4	2.9–11	116.5	2(3.5,5.5)	Yes	Shorting corresponding slots
Lakrit et al. 2019)	42 × 32 × 1.6 2150	FR4	2.7–14.9	138.6	2(3.5, 5.5)	Yes	1-PIN diode
Mohamed et al. 2017)	42 × 50 × 1.6 3360	FR4	3–11	114.2	2(6.1, 4.3)	Yes	1-Varactor
Mayuri 2020)	37.8 × 27.1 × 1.6 1639	FR4	3.17–11.61	114.2	2(3.5, 5.5)	Yes	6-PIN diodes
Elkorany et al. 2021)	60 × 41 × 1.6 3936	FR4	3–11	114.2	1(4)	Yes	3-Varactors
This work	20 × 24 × 0.787 377	FR4	2.7–11.4	123.4	2 (3.15, 5.35)	Yes	2–PIN diodes

NA not applicable

antenna must be arranged in a face-to-face configuration at a predetermined separation of 30 cm from each other for the time domain analysis, as shown in Fig. 13.

A time signal with a frequency spectrum in the UWB range can be used to evaluate the investigated antenna's time response. Fifth-order Gaussian monocycle signal is used as the input pulse for the time domain analysis of the studied antenna, which results in a typical UWB signal with a mid-frequency of 6.5 GHz. As illustrated in Fig. 13a–b that the radiated signal is nearly the same as the input signal, but in the case of mode 4, the radiated pulse exhibits some ringing characteristics.

Group delay can also be used to characterize the extent of distortion in the investigated filtenna. In a UWB system, a stable group delay with minimum non-uniformity is always preferable for the entire UWB range. Two similar antennas were arranged face-to-face and side by side with a separation of 30 cm in space for group delay simulation, and their group delay characteristics were studied for mode 3 and mode 4, as shown in Figs. 14 and 15.

It should be emphasized that the investigated UWB filtenna has nearly constant group delay throughout the UWB frequency range, with the exception of at the notch bands, making it an excellent practical solution. The presented antenna is therefore appropriate for UWB transmission since it has acceptable time domain properties and less signal distortion.

5 Performance Comparison of Presented Work With Existing Related Work

Table 4 compares the examined UWB filtenna's performance to that of other UWB antennas currently in use. It is evident from the table that the investigated filtenna has a compact size and deployed the least number of PIN diodes to realize reconfigurability in the notch bands.

6 Conclusion

A compact reconfigurable CPW-fed dual band-notch UWB filtenna using the two rectangular CSRR's deploying two PIN diodes has been examined and introduced in this letter. A patch with dual rectangular parasitic stubs, U- shaped aperture, and CPW feed has been employed to obtain optimum impedance matching throughout the UWB frequency spectrum of 2.7–11.4 GHz. The notch bands can be varied between the S-band (2.85–3.34 GHz) and WLAN (4.9–5.64 GHz) bands, respectively, by switching ON and OFF the PIN diodes. The investigated antenna's prototype is built, and the VSWR is measured and compared with simulated data. Very excellent agreement between them is achieved, and notch frequencies at 3.15 and 5.35 GHz are realized, respectively. The investigated filtenna has achieved a directional radiation pattern in the E-plane and

omnidirectional pattern in H-plane. In addition, the gain is decreased at notch frequencies. Throughout the UWB range, the group delay is approximately constant, with sharp variations at the notch frequencies. Thus, the compact size, stable frequency- and time-domain responses, high gain, and the presence of reconfigurable band-notches validate that the presented UWB filtenna is relevant for reconfigurable UWB applications.

References

Aboufoul T, Alomainy A, Parini C (2012) Reconfiguring UWB monopole antenna for cognitive radio applications using GAAS FET switches. IEEE Antennas Wirel Propag Lett 11:392–394. https://doi.org/10.1109/LAWP.2012.2193551

Alhegazi A, Zakaria Z, Shairi NA, Ibrahim IM, Ahmed S (2017) A novel reconfigurable UWB filtering-antenna with dual sharp band notches using double split ring resonators. Prog Electromagn Res C 79:185–198

Antonino-Daviu E, Cabedo-Fabrés M, Ferrando-Bataller M, Vila-Jimenez A (2007) Active UWB antenna with tunable band-notched behavior. Electron Lett 43(18):959–960. https://doi.org/10.1049/el:20071567

Bong HU, Jeong M, Hussain N, Rhee SY, Gil SK, Kim N (2019) Design of an UWB antenna with two slits for 5G/WLAN notched bands. Microw Opt Technol Lett 61(5):1295–1300. https://doi.org/10.1002/mop.31670

Changzhou Hua, Yunlong Lu, and Taijun Liu (2017) UWB Heart-Shaped Planar Monopole Antenna with a Reconfigurable Notched Band," Progress In Electromagnetics Research Letters 65:123–130 http://www.jpier.org/PIERL/pier.php?paper=16120203.

Costantine J, Tawk Y, Barbin SE, Christodoulou CG (2015) Reconfigurable Antennas: design and applications. Proc IEEE 103(3):424–437. https://doi.org/10.1109/JPROC.2015.2396000

De A, Roy B, Bhattacharjee AK (2020) Design and investigations on a compact, UWB, monopole antenna with reconfigurable band notches for 5.2/5.8 GHz WLAN and 5.5 GHz Wi-MAX bands. Int J Commun Syst 33(7):1–13. https://doi.org/10.1002/dac.4323

Elkorany AS, Ahmed GT, Mohamed HA et al (2021) Reconfigurable band notch butterfly-wing shaped ultra-wide band antenna using varactor diodes. Microsyst Technol 27:2695–2703

Emadian SR, Ahmadi-Shokouh J (2015) Very small dual band-notched rectangular slot antenna with enhanced impedance bandwidth. IEEE Trans Antennas Propag 63(10):4529–4534. https://doi.org/10.1109/TAP.2015.2456905

Federal Communications Commission (2002) Federal Communications Commission revision of Part 15 of the commission's rules regarding ultra-wideband transmission system from 3.1 to 10.6 GHz. ET-Docket, Washington, DC, USA

Galvan-Tejada GM, MA Peyrot-Solis, H Jardón-Aguilar (2015) UltraWideband Antennas: Design Methodologies, and Performance. CRC Press

Hammache B, Messai A, Messaoudene I, Denidni TA (2019) A compact ultrawideband antenna with three C-shaped slots for notched band characteristics. Microw Opt Technol Lett 61(1):275–279. https://doi.org/10.1002/mop.31535

Horestani AK, Shaterian Z, Naqui J, Martín F, Fumeaux C (2016) Reconfigurable and tunable s-shaped split-ring resonators and application in band-notched UWB antennas. IEEE Trans Antennas Propag 64(9):3766–3776. https://doi.org/10.1109/TAP.2016.2585183

Hu ZH, Hall PS, Kelly JR, Gardner P (2010) UWB pyramidal monopole antenna with wide tunable band-notched behavior. Electron Lett 46(24):1588–1590. https://doi.org/10.1049/el.2010.2839

Iqbal A, Smida A, Mallat NK, Islam MT, Kim S (2019) A compact UWB antenna with independently controllable notch bands. Sensors. https://doi.org/10.3390/s19061411

Jairath K, Singh N, Jagota V, Shabaz M (2021) Compact ultrawide band metamaterial-inspired split ring resonator structure loaded band notched antenna. Math Probl Eng. https://doi.org/10.1155/2021/5174455

Jiang W, Che W (2012) A novel UWB Antenna with dual notched bands for WiMAX and WLAN applications. IEEE Antennas Wirel Propag Lett 11:293–296. https://doi.org/10.1109/LAWP.2012.2190490

Kalteh AA, DadashZadeh GR, Naser-Moghadasi M, Virdee BS (2012) Ultra-wideband circular slot antenna with reconfigurable notch band function. IET Microw Antennas Propag 6(1):108–112. https://doi.org/10.1049/iet-map.2011.0125

Koteswara Rao Devana VN, Maheswara Rao A (2020) Design and analysis of dual band-notched UWB antenna using a slot in feed and asymmetrical parasitic stub. IETE J Res. https://doi.org/10.1080/03772063.2020.1816226

Lakrit S, Das S, El Alami A, Barad D, Mohapatra S (2019) A compact UWB monopole patch antenna with reconfigurable band-notched characteristics for Wi-MAX and WLAN applications. Int J Electron Commun (AEÜ). https://doi.org/10.1016/j.aeue.2019.04.001

Li Y, Li W, Ye Q (2014) A compact circular slot UWB antenna with multimode reconfigurable band-notched characteristics using resonator and switch techniques. Microw Opt Technol Lett 56(3):570–574. https://doi.org/10.1002/mop

Mayuri P, Rani ND, Subrahmanyam NB, Madhav BT (2020) Design and analysis of a compact reconfigurable dual band notched UWB antenna. Prog Electromagn Res C 98:141–153. https://doi.org/10.2528/PIERC19082903

Mohamed HA, Elkorany AS, Saad SA, Saleeb DA (2017) New simple flower shaped reconfigurable band-notched UWB antenna using single varactor diode. Prog in Electromagn Res C 76:197–206

Moradi N, Nazari F, Aliakbarian H, Namin FA (2022) Compact ultrawideband monopole antenna with continuously tunable notch band characteristics. Prog Electromagn Res C 118:71–81. https://doi.org/10.2528/PIERC21120207

Nikolaou S, Kingsley ND, Ponchak GE, Papapolymerou J, Tentzeris MM (2009) UWB elliptical monopoles with a reconfigurable band notch using MEMS switches actuated without bias lines. IEEE Trans Antennas Propag 57(8):2242–2251. https://doi.org/10.1109/TAP.2009.2024450

Oraizi H, Shahmirzadi NV (2017) Frequency- and time-domain analysis of a novel UWB reconfigurable microstrip slot antenna with switchable notched bands. IET Microw Antennas Propag 11(8):1127–1132. https://doi.org/10.1049/iet-map.2016.0009

Parameswari S, Chitra C (2021) Compact textile UWB antenna with hexagonal for biomedical communication. J Ambient Intell Human Comput. https://doi.org/10.1007/s12652-021-03228-3

Puri SC, Das S, Tiary MG (2020) UWB monopole antenna with dual-band-notched characteristics. Microw Opt Technol Lett 62(3):1222–1229. https://doi.org/10.1002/mop.32112

Ray KP (2008) Design aspects of printed monopole antennas for ultra-wide band applications. Int J Antennas Propag. https://doi.org/10.1155/2008/713858

Sarkar D, Srivastava KV, Saurav K (2014) A compact microstrip-fed triple band-notched UWB monopole antenna. IEEE Antennas

Wirel Propag Lett 13:396–399. https://doi.org/10.1109/LAWP.2014.2306812

Schantz H (2005) The art and science of ultra-wideband antennas. Artech House Inc, Norwood, MA

Sharma N, Bhatia SS (2019) Design of printed monopole antenna with band notch characteristics for ultra-wideband applications. Int J RF Microw Comput Aided Eng. https://doi.org/10.1002/mmce.21894

Shi M, Cui L, Liu H, Lv M, Sun X (2018) A new UWB antenna with band-notched characteristic. Prog Electromagn Res M 74:201–209. https://doi.org/10.2528/PIERM18081002

Sohail A, Alimgeer KS, Iftikhar A, Ijaz B, Kim KW, Mohyuddin W (2018) Dual notch band UWB antenna with improved notch characteristics. Microw Opt Technol Lett 60(4):925–930. https://doi.org/10.1002/mop

Sung Y (2013) Triple band-notched UWB planar monopole antenna using a modified H-shaped resonator. IEEE Trans Antennas Propag 61(2):953–957. https://doi.org/10.1109/TAP.2012.2223434

Ting Wu, Bai H, Li P, Shi X-W (2014) A simple planar monopole UWB slot antenna with dual independently and reconfigurable band-notched characteristics. Int J RF Microw Comput-Aided Eng 24(6):706–712. https://doi.org/10.1002/mmce

Valderas D, Sancho JI, Puente D, Lingan C, Chen X (2011) Ultrawideband antennas design and applications, london. Imperial College Press, U.K.

Vallappil AK, Khawaja BA, Rahim MKA, Iqbal MN, Chattha HT, Ali MFBM, (2022) A compact triple-band UWB inverted triangular antenna with dual-notch band characteristics using SSRR metamaterial structure for use in next-generation wireless systems. Fractal Fract. https://doi.org/10.3390/fractalfract6080422

Zhao D, Lan L, Han Y, Liang F, Zhang Q, Wang BZ (2014) Optically controlled reconfigurable band-notched UWB antenna for cognitive radio applications. IEEE Photonics Technol Lett 26(21):2173–2176. https://doi.org/10.1109/LPT.2014.2349961